Simplified method for settlement prediction of single pile and pile group using a hyperbolic model

Qian-qing Zhang[1],*, Shu-cai Li[2], Fa-yun Liang[3], Min Yang[4], Qian Zhang[5]

Abstract

A simplified approach for nonlinear analysis of the load-displacement response of a single pile and a pile group is presented using the load-transfer approach. A hyperbolic model is used to capture the relationship between unit skin friction and pile-soil relative displacement developed at the pile-soil interface and the load-displacement relationship developed at the pile end. As to the nonlinear analysis of the single pile response, a highly effective iterative computer program is developed using the proposed hyperbolic model. Furthermore, determinations of the parameters related to the hyperbolic model of an individual pile in a pile group are obtained considering interactions between piles. Based on the determinations of the parameters presented in the hyperbolic model of an individual pile in a pile group and the proposed iterative computer program developed for the analysis of the single pile response, the conventional load-transfer approach can then be extended to the analysis of the load-settlement response of an arbitrary pile in a pile group. Comparisons of the load-settlement response demonstrate that the proposed method is generally in good agreement with the field-observed behavior and the calculated results derived from other approaches.

Keywords: Single pile, Pile group, Skin friction, End resistance, Settlement, A hyperbolic model.

1. Introduction

A number of theoretical methods have been used for the analysis of a single pile, including the theoretical load-transfer curve method (Kraft et al. [1]; Zhang et al. [2]), the shear displacement method (Randolph and Wroth [3]; Guo and Randolph [4]), the finite-element method (Tosini et al. [5]), and other simplified analytical methods (Castelli and Motta [6]; Zhang and Zhang [7]).

In most of the available prediction approaches, the pile group settlement is related to the settlement of a single pile.

* Corresponding author: zhangqq@sdu.edu.cn

1 Ph.D, Geotechnical and Structural Engineering Research Center, Shandong University, Jinan, China; Key Laboratory of Geotechnical and Underground Engineering (Tongji University), Ministry of Education, Shanghai, China; State Key Laboratory for Geo Mechanics and Deep Underground Engineering, China University of Mining and Technology, Xuzhou, China

2 Professor, Geotechnical and Structural Engineering Research Center, Shandong University, Jinan, China

3 Professor, Key Laboratory of Geotechnical and Underground Engineering (Tongji University), Ministry of Education, Shanghai, China

4 Professor, Key Laboratory of Geotechnical and Underground Engineering (Tongji University), Ministry of Education, Shanghai, China

5 Ph.D. Candidate, Geotechnical and Structural Engineering Research Center, Shandong University, Jinan, China

However, the mechanism of load transfer in pile group is different from that in a single pile due to interaction of piles, surrounding soils and pile cap.

The interactive effects between piles should be taken into account when the calculated approaches for the single pile response are extended to the analysis of the behavior of pile group. To account for the interaction between piles, the interaction factor defined for two equally loaded identical piles as the ratio of the increase in settlement of a pile due to an adjacent pile to the settlement of a single pile due to its own load was first introduced by Poulos [8], who showed that pile group effects can be assessed by superimposing the effects of two pile. Numerous subsequent studies (Lee [9]; Comodromos and Bareka [10]; Zhang et al. [2]) have been conducted using the simplified concept of interaction factors. It has been recognized that the conventional interaction factor approach tends to exaggerate the interactive effects between piles in a group, thereby leading to an overestimation of the pile settlement, as reported by Mylonakis and Gazetas [11], and Chen et al. [12]. Therefore, for the further prediction of pile group settlement, it is necessary to revisit the interaction factor problem between two vertically loaded piles. However, it is rather unlikely that the two-pile interaction factor approach will be readily applied to the problems of a large pile group due to large computational requirements.

In practical applications, the load-transfer approach presented by Coyle and Reese [13] is an efficient method

for single-pile analysis. In this method, the load-transfer functions are required to describe the relationship between the mobilized unit skin friction and the pile movement. Such a load-transfer function concept was first developed by Seed and Reese [14], after which many other researchers (Kezdi [15]; Armaleh and Desai [16]; Hirayama [17]; Lee and Xiao [18]; Zhang and Zhang [7]) proposed various forms of load-transfer functions. To account for the non-linearity in the stress-displacement response of soil, a hyperbolic model is commonly used to capture the relationship between unit skin friction and pile-soil relative displacement developed along the pile-soil interface and the load-displacement relationship developed at the pile end (the capability of the hyperbolic model will be demonstrated in a later section). However, the conventional load-transfer approaches are rather difficult to extend to the analysis of a pile group.

To provide a rapid predication of the response characteristics of a single pile and a pile group, a hyperbolic model is adopted to simulate the load-displacement response of both the pile base and the shaft. Based on the proposed hyperbolic model, a highly effective iterative computer program is developed for the nonlinear analysis of the response of a single pile and an arbitrary pile in a pile group. Two well-documented field test results and the calculated results derived from other approaches will then be investigated to verify the efficiency and accuracy of the present method for the analysis of the response of a single pile and a pile group.

2. Analysis of the Response of a Single Pile

The load-settlement response of an axially loaded pile depends on the compressibility of the pile, the relationship between skin friction and pile-soil relative displacement developed at the pile-soil interface, and the load-displacement response developed at the pile tip soil. In this paper, the soil continuum is idealized as a number of separate horizontal layers, each with its own load transfer curve. The pile is then idealized as a series of elastic elements supported by discrete vertical springs at the ends of each pile segment, which represent the skin resistance along the pile-soil interface, and a spring at the pile tip representing the end-bearing resistance of the soil (see Fig. 1). In order to account for non-linearity in the stress-strain response of soil, the load-displacement response of both the pile base and the shaft are taken to be hyperbolic (see Figs. 2 and 3, respectively). To define the shaft response, the ultimate unit skin friction and the initial gradient of the response are required, whereas the ultimate unit end resistance and the initial gradient of the base response are required to assess the load-displacement response of the pile base.
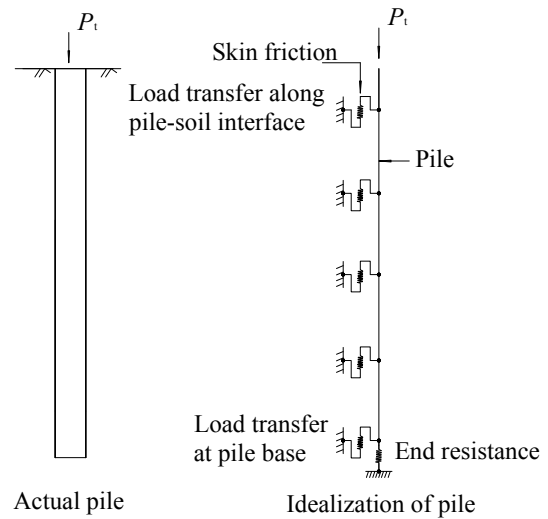
Fig. 1 Idealization of pile in load-transfer analysis

$$\frac{\tau_s}{\tau_{su}} = \frac{\dfrac{S_s}{S_{su}}}{0.01087 + 1.05091\dfrac{S_s}{S_{su}}} \quad R^2 = 0.8376$$
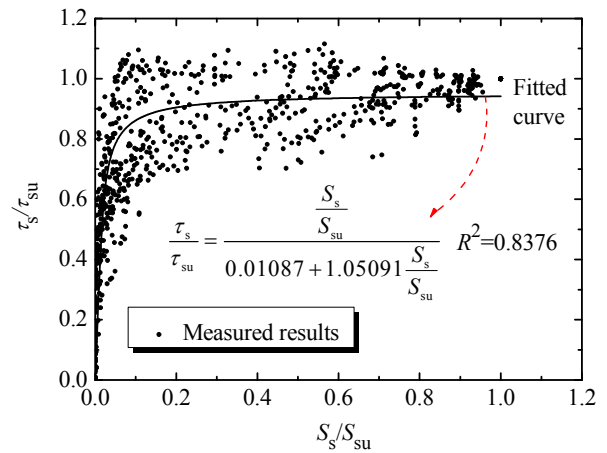
Fig. 2 Observed and theoretical relationship between τ_s/τ_{su} and S_s/S_{su} for instrumented piles

$$\frac{\tau_b}{\tau_{bu}} = \frac{\dfrac{S_b}{S_{bu}}}{0.04534 + 1.06149\dfrac{S_b}{S_{bu}}} \quad R^2 = 0.8121$$
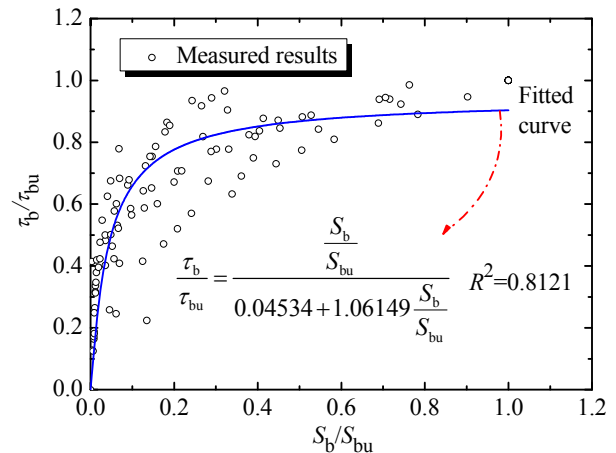
Fig. 3 Observed and theoretical relationship between τ_b/τ_{bu} and S_b/S_{bu} for piles

2.1. Hyperbolic model of skin friction

To verify the reliability of the hyperbolic model of skin friction, results of the load tests on 7 instrumented piles conducted by Yang et al. [19], and Zhang et al. [20, 21] are adopted, as shown in Fig.2. Brief descriptions of the 7 test piles are given in Table 1. In Fig. 2, the measured results of skin friction can be calculated by dividing the difference of two consecutive axial forces by the pile shaft area between the two groups of strain gauges. As to the measured pile-soil relative deformation, an assumption is made herein that pile-soil relative slip does not occur for practical purposes, and the displacement of the soils around pile is assumed to be identical to the pile shaft displacement. The measured data derived from the strain gauges can reflect the differences between the displacement of the soils around pile and the pile displacement. Therefore, the pile displacement at a given depth derived from equation (1) can be called the pile-soil relative displacement. Actually, the measured pile-soil relative displacement at a given depth is the pile displacement at that depth. It is commonly used equation (1) to estimate the relative displacement between soil and pile segment i, S_{si}, in practical applications (Zhang et al. [22]):

$$S_{si} = S_t - \sum_{j=1}^{i} \frac{L_j}{2} \left(\varepsilon_j + \varepsilon_{j+1} \right) \tag{1}$$

Table 1 Brief details of test piles

Reference	Pile No.	Pile type	Soil distributed along pile	Pile length (m)	Pile diameter (m)
Yang et al. [19]	PJ1	Jacked steel H-pile	Fill, alluvium and completely decomposed granite	40.9	/
	PD2	Driven steel H-pile	Fill, alluvium and completely decomposed granite	39.6	/
Zhang et al. [20]	S1	Bored pile	Silt, clay, silty sand with silty clay, completely decomposed bedrock, highly decomposed bedrock, and moderately decomposed bedrock	119.9	1.1
	S2	Bored pile	Silt, clay, clay with silty clay, completely decomposed bedrock, highly decomposed bedrock, and moderately decomposed bedrock	88.2	1.1
	S3	Bored pile	Silt, clay, clay with silty clay, completely decomposed bedrock, highly decomposed bedrock, and moderately decomposed bedrock	88.4	1.1
Zhang et al. [21]	S1#	Bored pile	Clay, muddy clay, fine sand with mud, mud, fine sand, gravel, silty clay, completely decomposed diorite, highly decomposed diorite, and moderately decomposed diorite	109.7	1.1
	S3#	Bored pile	Clay, muddy clay, fine sand with mud, mud, fine sand, gravel, silty clay, completely decomposed diorite, highly decomposed diorite, and moderately decomposed diorite	103.7	1.1

where L_j is the length of pile segment j; S_t is the pile head settlement, which can be derived from the dial gauges installed at the pile top; and ε_j is the strain of the reinforcing steel bar located at pile section j, which is obtained using the strain gauges attached to the steel rebar.

Fig. 2 contains 808 data points and presents the observed relationship between the unit skin friction and the pile-soil relative displacement with the unit skin friction, τ_s, normalized by the limiting unit shaft resistance, τ_{su}, and the measured pile-soil relative deformation, S_s, normalized by the measured pile-soil relative displacement at the ultimate skin friction, S_{su}.

It is well known that the relationship between the skin friction and the corresponding shear displacement follows a softening model when the skin friction is fully mobilized. However, Fig.2 suggests that a hyperbolic model can be used to approximately simulate the relationship between τ_s/τ_{su} and S_s/S_{su} irrespective of soil types, stratigraphy, and loading procedure, and has a high accuracy ($R^2=0.8376$).

The relationship between unit skin friction and its corresponding shear deformation can be approximated by a hyperbolic equation having the following form (see Fig.2):

$$\tau_s = \frac{S_s}{a + bS_s} \tag{2}$$

where a and b are empirical coefficients; S_s is the relative displacement along the pile-soil interface; and τ_s is the shaft shear stress. The physical meaning and determination of the parameters a and b will be discussed later.

As to the shear displacement method, an assumption is made that slip does not occur at the pile-soil interface, and the displacement of the soils around pile is assumed to be identical to the pile shaft displacement. Therefore, the pile shaft displacement induced by the shaft shear stress can be calculated with the elastic solution as suggested by Randolph and Wroth [3]:

$$S_s = \frac{\tau_s r_0}{G_s} \ln \left(\frac{r_m}{r_0} \right) \tag{3}$$

where G_s is the soil shear modulus; r_0 is the pile radius; and r_m is the radial distance from the pile center to a point at which the shaft shear stress induced by the pile can be

negligible.

For the pile embedded into multilayered soils, the value of G_s can be calculated by:

$$G_s = \frac{\sum_{i=1}^{n_s} G_{si} h_i}{L} \tag{4}$$

where G_{si} is the shear modulus of soil layer i around pile; h_i is the thickness of soil layer i; L is the pile length; and n_s is the number of soil layer.

According to Randolph and Wroth [3], in homogenous soils the value of r_m can be taken as:

$$r_m = 2.5L(1 - \upsilon_s) \tag{5}$$

where υ_s is the Poisson's ratio of soil around pile.

In arbitrarily layered soils, a modified expression for r_m can be written as follows:

$$r_m = 2.5L\rho_m(1 - \upsilon_{sa}) \tag{6}$$

where ρ_m is the modified inhomogeneity factor; and υ_{sa} is the average value of the Poisson's ratio of soils around pile. The values of ρ_m and υ_{sa} can be calculated in the following forms, respectively:

$$\rho_m = \frac{\sum_{i=1}^{n_s} G_{si} h_i}{G_{sm} L} \tag{7}$$

$$\upsilon_{sa} = \frac{\sum_{i=1}^{n_s} \upsilon_{si} h_i}{L} \tag{8}$$

where G_{sm} is the maximum shear modulus in the soil layers; and υ_{si} is the Poisson's ratio of soil layer i around pile.

The spring stiffness of soils around pile, k_s, can be calculated by:

$$k_s = \frac{\tau_s}{S_s} = \frac{G_s}{r_0 \ln\left(\dfrac{r_m}{r_0}\right)} \tag{9}$$

Therefore, the value of a can be obtained using the following equation:

$$a = \frac{1}{k_s} = \frac{r_0}{G_s} \ln\left(\frac{r_m}{r_0}\right) \tag{10}$$

The reciprocal of coefficient b can be taken as the unit skin friction at a very large value of the pile-soil relative displacement. This asymptote shaft resistance, τ_f, is slightly greater than the maximum possible value at the pile-soil interface, τ_{su}. It is convenient to express τ_f in terms of τ_{su} by means of a failure ratio, R_{sf}, as in the following:

$$\tau_{su} = R_{sf}\tau_f \tag{11}$$

The values of R_{sf} are found to be in the range 0.8 to 0.95 as suggested by Clough and Duncan [23].

In the analytical approach, the limiting unit skin friction τ_{su} is commonly determined based on a formula using soil parameters derived from both laboratory and in situ tests. The effective stress method is employed to predict τ_{su} in the drained condition. The following equation can be used to calculate the value of τ_{su}:

$$\tau_{su} = K\sigma_v' \tan\delta \tag{12}$$

where K is the lateral earth pressure coefficient; σ_v' is the effective overburden pressure at the depth under consideration; and δ is the friction angle of the pile-soil interface. For practical purposes, it is commonly assumed to be equal to the angle of shearing resistance of the surrounding soil, φ. The value of K depends on various factors including soil state, pile installation method, and pile geometry, and is related to the in situ earth pressure coefficient, K_0, whose value is approximately estimated by $K_0 = 1 - \sin\varphi$. Therefore, equation (12) can be written in another form (Yang et al. [19]):

$$\tau_{su} = K_0 \left(\frac{K}{K_0}\right) \tan\left[\varphi\left(\frac{\delta}{\varphi}\right)\right] \sigma_{vz}' \tag{13}$$

Suggested values of lateral earth pressure coefficient, K, and friction angle of the pile-soil interface, δ, are summarized in Table 2.

The value of b can then be calculated by:

$$b = \frac{1}{\tau_{sf}} = \frac{R_{sf}}{\tau_{su}} = \frac{R_{sf}}{K_0 \left(\dfrac{K}{K_0}\right) \tan\left[\varphi\left(\dfrac{\delta}{\varphi}\right)\right] \sigma_{vz}'} \tag{14}$$

2.2. Hyperbolic model of end resistance

Results of the load tests on 14 instrumented piles (Ji and Feng [29]; Bi et al. [30]; Zhang et al. [31]; Yang et al. [19]; Yao et al. [32]; Cheng et al. [33]) are used to assess the reliability of the hyperbolic model of end resistance, as shown in Fig.3. Brief descriptions of the 14 test piles are given in Table 3.

Table 2 Suggested values of K and δ

Suggested values of K and δ	Pile-soil condition	Reference
K/K_0=0.7-1.2	Smooth steel pipe piles, H-piles or concrete piles (Small-displacement piles)	Kulhawy [24]
K/K_0=1.0-2.0	Smooth steel pipe piles, H-piles or concrete piles (Large displacement piles)	Kulhawy [24]
K/K_0=1.0	Driven or jacked open-ended steel pile piles, Normally consolidated soil	Miller and Lutenegger [25]
K/K_0=1.0-4.0	Driven or jacked open-ended steel pile piles, Overconsolidated clay	Miller and Lutenegger [25]
K/K_0=1.2-1.5	Driven steel pile, Alluvium and completely decomposed granite	Yang et al. [19]
δ=(0.5-0.7)φ	Smooth steel pipe piles or H-piles	Kulhawy [24]
δ=(0.8-1.0)φ	Smooth concrete piles	Kulhawy [24]
δ=29.4°	Pipe pile, Dense sand	O'Neill and Raines [26]
δ=(21.3-31.6)°	Concrete pile, Clay and silt	Liu and Zhu [27]
δ=(28-30)°	Driven pile, Sand	Jardine et al. [28]
δ=(0.7-0.9)φ	Driven steel pile, Alluvium and completely decomposed granite	Yang et al. [19]

Table 3 Brief details of test piles

Reference	Pile No.	Pile type	Soil at pile base	Pile length (m)	Pile diameter (m)
Ji and Feng [29]	2	Bored pile	Limestone	81.5	1.0
Bi et al. [30]	1	Bored pile	Middle-sized coarse sand and cobblestone	110	2.5
	2	Bored pile	Middle-sized coarse sand and cobblestone	110	2.5
Zhang et al. [31]	SZ1	Bored pile	Gravel	76.2	0.8
	SZ2	Bored pile	Clay	59.3	0.8
Yang et al. [19]	PD2	Driven steel H-pile	Completely decomposed granite	39.6	/
	PD7	Driven steel H-pile	Completely to highly decomposed granite	45.1	/
	PJ1	Jacked steel H-pile	Completely decomposed granite	40.9	/
	PJ6	Jacked steel H-pile	Completely decomposed granite	39.0	/
	PJ7	Jacked steel H-pile	Completely decomposed granite	40.5	/
Yao et al. [32]	y1	Bored pile	Moderately decomposed mud rock	70	2.0
Cheng et al. [33]	S1	Bored pile	Fine sand	84	1.5
	SZ4	Bored pile	Fine sand	125	2.5
	N3	Bored pile	Coarse sand	76	1.5

Fig.3 contains 108 data points and presents the observed relationship between the unit end resistance and the pile base displacement with the unit end resistance, q_b, normalized by the ultimate unit end resistance, q_{bu}, and the measured pile end deformation, S_b, normalized by the measured pile base displacement at the ultimate end resistance, S_{bu}.

Fig.3 suggests that a hyperbolic model can be used to describe the relationship between q_b/q_{bu} and S_b/S_{bu} irrespective of soil types, stratigraphy, and loading procedure, and has a high accuracy (R^2=0.8121).

A hyperbolic model can be used to describe the relationship between unit end resistance and pile base displacement. This hyperbolic relationship can be described by the following equation (see Fig.3):

$$q_b = \frac{S_b}{f + gS_b} \tag{15}$$

where f and g are empirical coefficients, whose values

will be discussed later; S_b is the pile base load; and q_b is the unit end resistance;.

In the hyperbolic model of the soil below the pile base, the parameters f and g are required to define the load-displacement response at the pile end. The value of the initial gradient of the base response, k_b, may be conveniently expressed using the following equation as suggested by Randolph and Wroth [3]:

$$k_b = \frac{4G_b}{\pi r_0 \left(1 - \upsilon_b\right)} \tag{16}$$

The value of f can be taken as the reciprocal of k_b. That is:

$$f = \frac{1}{k_b} = \frac{\pi r_0 \left(1 - \upsilon_b\right)}{4G_b} \tag{17}$$

where G_b and υ_b are the shear modulus and Poisson's

ratio of the soil below the pile base, respectively.

The reciprocal of coefficient g can be taken as the unit end resistance at a very large value of the pile base deformation. One obtains:

$$g = \frac{1}{q_{bf}} = \frac{R_{bf}}{q_{bu}} \qquad (18)$$

where R_{bf} is a failure ratio of end resistance.

The ultimate unit end resistance, q_{bu}, can be calculated in the following form:

$$q_{bu} = N_q \sigma'_{vb} \qquad (19)$$

where N_q is a bearing capacity factor, whose value can be determined by its relationship with the angle of shearing resistance of the surrounding soil, φ; and σ'_{vb} is the vertical effective overburden pressure at the pile base.

2.3. Algorithm for load-settlement analysis of a single pile embedded in layered soils

Based on the proposed hyperbolic models, the theoretical method for a single pile embedded in multilayered soils can be analyzed with the following procedure.

(1) Assume a single pile is divided into n segments from the pile head to the pile end.

(2) Assume a small pile end settlement, S_{bn}.

(3) Calculate the mobilized pile base load, P_{bn}, using equation (15) and the assumed pile base displacement, S_{bn}.

(4) A vertical movement, S_{cn}, at the middle height of pile segment n is assumed (for the first trial, assume $S_{cn}=S_{bn}$). Based on the load transfer function as given in equation (2), the unit skin friction of pile segment n, τ_{sn}, can be obtained using the assumed value of S_{cn}.

(5) The load at the top of pile segment m, P_{tm}, can then be calculated as:

$$P_{tn} = P_{bn} + \pi d L_n \tau_{sn} \qquad (20)$$

where d is the pile diameter; and L_n is the length of pile segment n.

(6) Assuming a linear variation of load in the pile segment n, the elastic deformation at the midpoint of pile segment n, S_{cn}, can be calculated by:

$$S_{cn} = \left(\frac{P_{tn} + P_{bn}}{2} + P_{bn} \right) \left(\frac{0.5 L_n}{2 E_p A_p} \right) \qquad (21)$$

(7) The updated midpoint displacement of segment n, S'_{cn}, can be written as:

$$S'_{cn} = S_{bn} + S_{cn} \qquad (22)$$

(8) Compare the updated midpoint displacement S'_{cn}

with the assumed value of S_{cn} from step 4. If the computed displacement S'_{cn} does not agree with S_{cn} within a specified tolerance, e.g., 1×10^{-6} m, use S'_{cn} as the new value of S_{cn}. Repeat steps 4 to 8 until the value of $(S_{cn}-S'_{cn})$ is within the assumed tolerance.

(9) Calculate the load and displacement at the top of pile segment n, P_{tn} and S_{tn}, respectively, using the following form:

$$S_{tn} = S_{bn} + S'_{cn} \qquad (23)$$

$$P_{tn} = P_{bn} + \pi d L_n \tau'_{sn} \qquad (24)$$

where τ'_{sn} is derived from equation (2) and an updated midpoint displacement, $S'_{cn.}$

(10) Repeat steps 4 to 10 from pile segment n to pile segment 1 until the load-settlement relationship developed at the pile head is obtained.

(11) The procedure from steps 2 to 10 is then repeated using a different assumed pile end settlement, S_{bn}, until a series of load-displacement values are obtained.

The proposed simple analytical approach is economical and efficient, and suitable for the analysis of a single pile using different forms of load-transfer functions.

3. Case Studies on Single Pile Response

Two case histories reported in literature (O'Neill et al. [34]; Briaud et al. [35]) performed on single pile are used to check the reliability of the previously proposed method for the analysis of the load-settlement response of a single pile.

3.1. Case one

The first case history analyzed, regarding the loading test, was reported by O'Neill et al. [34] on a closed-ended steel pipe pile in stiff overconsolidated clays. The pile had an external radius of 137 mm with a wall thickness of 9.3 mm, and was driven to a penetration of 13.1 m. Nine of the piles were installed in a 3×3 configuration with a center-to-center spacing r=3d, while each of the two remaining piles were located some 3.7 m from the center of the group on opposite sides of the group. The nine-pile group was connected to a rigid reinforced concrete block. The two single piles and the nine-pile group were loaded to failure after the final nine-pile test, a five-pile subgroup and a four-pile subgroup were tested.

According to the soil properties evaluated by back analysis (Castelli and Maugeri [36]), the soil compression modulus back calculated from the test results was taken as 195 MPa, the ultimate end bearing capacity was 130 kN, and the elastic modulus for the steel pipe pile was adopted as 210 GPa. A linearly increasing undrained shear strength profile was considered. The unit shaft resistance was assumed to be 19 kPa at the surface increasing linearly to 93 kPa at the pile base.

In the analysis of the response of a single pile, the single pile is divided into 13 segments with each pile segment of 1.0 m in length, except of the pile end segment

where the pile segment length is assumed to be 1.1 m. In practice, the ultimate unit skin friction of each pile segment can be adopted as an average value of the limiting shaft resistance of a recommended soil depth, as shown in Fig. 4. The Poisson's ratio of the soil is adopted as 0.5. The value of R_{sf} is adopted as 0.80, 0.90 and 0.95 for the whole deposit, respectively, whereas the value of R_{bf} is assumed to be 0.90 and 0.95 for the soil below the pile toe, respectively. The values of a and b are calculated using equations (10), and (14), respectively, while the values of f and g can be computed by equations (17) and (18), respectively.
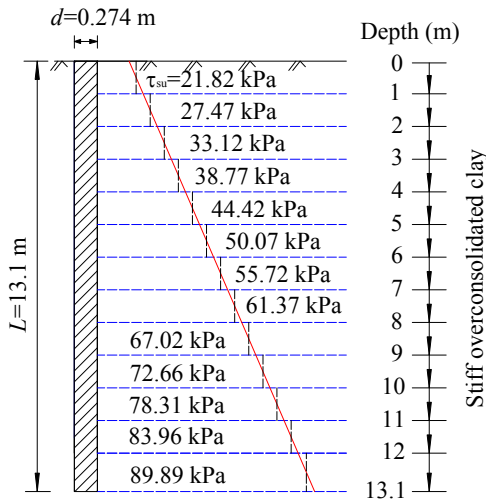
Fig. 4 Calculated value of limiting unit skin friction of soils around each pile segment

Comparisons between the measured single pile load-settlement curve given by O'Neill et al. [34] and the computed single pile response derived from the present method and the approach presented by Castelli and Maugeri [36] are shown in Fig. 5.
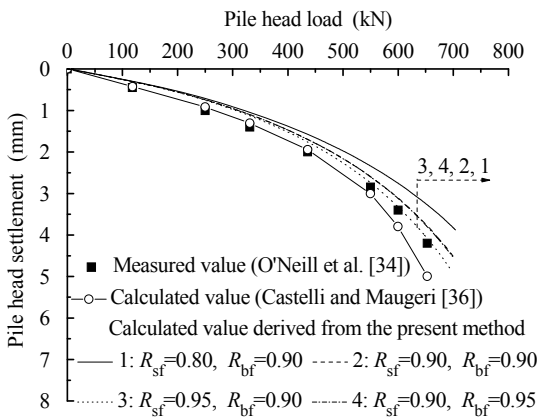
Fig. 5 Measured and calculated load-settlement curves at the pile head of a single pile

Fig. 5 shows that at low loading level, the load-displacement curve at the pile head plotted from the

present approach is generally consistent with the measured results given by O'Neill et al. [34] and the calculated values presented by Castelli and Maugeri [36]. At high load level, the measured displacements and the calculated values reported by Castelli and Maugeri are slightly larger than the calculated values derived from the present method. It also can be concluded that the pile head displacement estimated from the present approach increases with increasing failure ratio of skin friction, R_{sf}, and end resistance, R_{bf}, at the same loading level.

3.2. Case two

The second case history analyzed, regarding the loading test, reported by Briaud et al. [35] was performed on a five-group in a medium dense sand together with a control single pile as a reference. The 9.15-m-long piles were closed-ended steel pipe piles, and had 273 mm in outside diameter and 9.3 mm in wall thickness. The five piles were connected by a rigid reinforced concrete cap with a center-to-center spacing $r=3d$. A value of 38.3 MPa was reported for the shear modulus of the dense sand and the elastic modulus for the steel pipe pile was taken as 210 GPa (Briaud et al. [35]). As suggested by Castelli and Maugeri [36], at this test site, the analysis of the single pile behavior was conducted considering a linearly increasing unit skin friction ranging from zero at the ground surface up to 45 kPa at the pile base, and the ultimate end bearing capacity was 120 kN.

In the analysis of case two, the single pile is divided into 10 segments with each pile segment of 1.0 m in length, except of the pile end segment where the pile segment length is assumed to be 0.15 m. In practice, the ultimate unit skin friction of each pile segment can be adopted as an average value of the limiting shaft resistance of a recommended soil depth, as shown in Fig. 6.
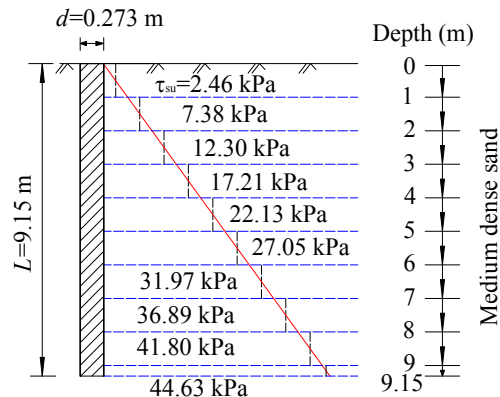
Fig. 6 Calculated value of limiting unit skin friction of soils around each pile segment

The Poisson's ratio of the soil is adopted as 0.5. The value of R_{sf} is adopted as 0.80, 0.90 and 0.95 for the whole deposit, respectively, whereas the value of R_{bf} is assumed to be 0.90 and 0.95 for the soil below the pile toe, respectively. The values of a and b are calculated using equations (10), and (14), respectively, while the values of f

Qian-qing Zhang, Shu-cai Li, Fa-yun Liang, Min Yang, Qian Zhang

and g can be computed by equations (17) and (18), respectively.

Fig.7 shows that the calculated results estimated from the present approach is generally in good agreement with the measured values given by Briaud et al. [35] and the computed results suggested by Castelli and Maugeri [36]. As discussed previously, the pile head displacement estimated from the present approach increases with increasing failure ratio of skin friction, R_{sf}, and end resistance, R_{bf}, at the same loading level.
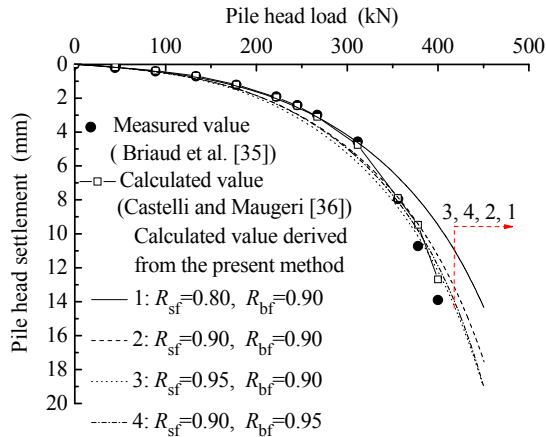
Fig. 7 Measured and calculated load-settlement curves at the pile head of a single pile

4. Developing a Load-Transfer Function for a Pile Group

A hyperbolic model, general used in the analysis of the behaviors of single piles, is extended to analyze the response of a pile group by accounting for the interaction between individual piles. In this work, the interactive effects between the pile shaft and pile base are assumed to be uncoupled, the shaft and base interactions are thereby considered separately for individual piles in a pile group. This simplified consideration is consistent with the hybrid-layer approach as proposed by Lee [9] and the method given by Lee and Xiao [18].

4.1. Determinations of the parameters related to the hyperbolic model of skin friction of an individual pile in a pile group

Consider two piles, i and j, as shown in Fig.8. Assume the pile-soil relative slip does not occur, and the displacement of the soils around pile is assumed to be identical to the pile shaft displacement. Based on the formulation presented by Randolph and Wroth [3], the vertical displacement of the soil surrounding pile i, S_{sij}, induced by the shaft shear stress of pile j, τ_{sj}, can be written as:

$$S_{sij} = \frac{\tau_{sj} r_0}{G_s} \ln\left(\frac{r_m}{r_{ij}}\right) \qquad (25)$$
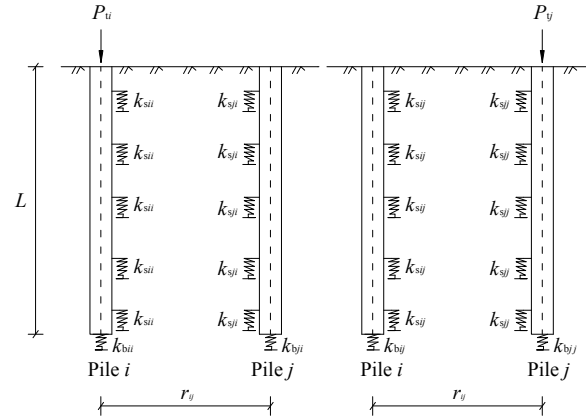
Fig. 8 Interaction between two piles

where r_m is the limiting radius of influence of the loaded pile. r_m can be taken as identical to the value adopted for a single pile, as suggested by Lee and Xiao [18]. This is because the value of r_m is only used to calculate the potential influence of elastic soil displacement induced by an individual pile on the nearby piles within the influence zone. Outside r_m, no pile interaction is considered.

For a group of n_p piles, the vertical displacement of the soil surrounding pile i, S_{sij}, induced by the shaft shear stress of pile j, τ_{sj} (j=1 to n_p, and $j{\neq}i$) can be written as:

$$S_{sij} = \sum_{j=1, j\neq i}^{n_p} \frac{\tau_{sj} r_0}{G_s} \ln\left(\frac{r_m}{r_{ij}}\right) \qquad (26)$$

To developing a simplified solution procedure, the shaft shear stress at a given depth in equation (26) is assumed to be the same for all piles in the group. The justification of such an important simplification has been discussed by Lee and Xiao [18]. Therefore, the variation of spring stiffness of the soils around pile i, k_{sij}, due to the shaft shear stress, τ_{sj} (j=1 to n_p, and $j{\neq}i$), can be written in the following form (see Fig.8):

$$k_{sij} = \sum_{j=1, j\neq i}^{n_p} \frac{G_s}{r_0 \ln\left(\dfrac{r_m}{r_{ij}}\right)} \qquad (27)$$

The shaft shear stress of pile j, τ_{sji}, induced by the spread of the shaft shear stress of pile i, τ_{si}, can be expressed by:

$$\tau_{sji} = \frac{\tau_{si} r_0}{r_{ij}} \qquad (28)$$

For pile j, τ_{sji} can be taken as a negative skin friction which pulls pile j down, whereas pile j generates a counter force with the same value but opposite direction namely τ_{sij}', which may reduce the vertical displacement of the soil

around pile i. The vertical displacement of the soil surrounding pile i, S'_{sij}, induced by the shaft shear stress, τ'_{sij}, can then be calculated as:

$$S'_{sij} = \frac{\tau_{sji} r_0}{G_s} \ln\left(\frac{r_m}{r_{ij}}\right) = \frac{\tau_{si} r_0^2}{G_s r_{ij}} \ln\left(\frac{r_m}{r_{ij}}\right) \tag{29}$$

Following the above assumption that the shaft shear stress, τ_{sj}, ($\tau_{sj}=\tau_{si}$, $j=1$ to n_p) at a given depth is assumed to be the same for all piles in the group, the vertical displacement of the soil surrounding pile i, S'_{sij}, induced by the shaft shear stress, τ'_{sij} ($j=1$ to n_p, and $j \neq i$), can be written as:

$$S'_{sij} = \sum_{j=1, j \neq i}^{n_p} \frac{\tau_{sj} r_0^2}{G_s r_{ij}} \ln\left(\frac{r_m}{r_{ij}}\right) \tag{30}$$

The variation of spring stiffness of soils around pile i, k'_{sij}, induced by the shaft shear stress, τ'_{sij} ($j=1$ to n_p, and $j \neq i$), can then be written by:

$$k'_{sij} = \sum_{j=1, j \neq i}^{n_p} \frac{G_s r_{ij}}{r_0^2 \ln\left(\dfrac{r_m}{r_{ij}}\right)} \tag{31}$$

The total equivalent spring stiffness of the soils around pile i, k_{si}, can be expressed in the following form:

$$\frac{1}{k_{si}} = \frac{1}{k_{sii}} + \frac{1}{k_{sij}} - \frac{1}{k'_{sij}} \tag{32}$$

where k_{sii} is the spring stiffness of soils around pile i due to its own loading, which can be calculated using equation (9).

The reciprocal of the initial elastic soil stiffness along the pile-soil interface of an individual pile i in an n_p-pile group, a_g, can be written as:

$$a_g = \frac{1}{k_{si}} \tag{33}$$

The value of parameter, b_g, related to the hyperbolic model of skin friction of an individual pile i in an n_p-pile group can be taken as identical to the value of b of a hyperbolic model of skin friction of a single pile derived from equation (14).

4.2. Determinations of the parameters related to the hyperbolic model of end resistance of an individual pile in a pile group

At some distance from the pile base, the loading will appear as a point load. The settlement, $S_b(r)$, around a point load decreases inversely with the radius r and is given by (Randolph and Wroth [3]):

$$S_b(r) = \frac{q_b (1 - \upsilon_b)}{2\pi r G_b} \tag{34}$$

For a group of n_p piles, the interactive effects of the displacement induced on the base of pile i can be established by the principle of superposition. Thus, the displacement at the base of pile i, $S_{bij}(r_{ij})$, induced by the vertical load developed at the base of other (n_p-1) piles can be written as:

$$S_{bij}(r_{ij}) = \frac{(1 - \upsilon_b)}{2\pi G_b} \sum_{j=1, j \neq i}^{n_p} \frac{q_{bj}}{r_{ij}} \tag{35}$$

where r_{ij} is the center to center distance between pile i and pile j; and q_{bj} is the vertical displacement developed at the base of pile j.

The end resistance, q_{bj} ($j=1$ to n_p), in equation (35) is assumed to be the same for all piles in the n_p-pile group. The variation of soil stiffness at the base of pile i, k_{bij}, induced by the end resistance, q_{bj} ($j=1$ to n_p, and $j \neq i$), can be written as (see Fig.8):

$$k_{bij} = \frac{2\pi G_b}{(1 - \upsilon_b) \displaystyle\sum_{j=1, j \neq i}^{n_p} \frac{1}{r_{ij}}} \tag{36}$$

Thus, the total equivalent soil stiffness at the base of pile i, k_{bi}, can be calculated by:

$$\frac{1}{k_{bi}} = \frac{1}{k_{bii}} + \frac{1}{k_{bij}} \tag{37}$$

where k_{bii} is the soil stiffness at the base of pile i induced by its own loading, which is derived from equation (16).

The reciprocal of the initial elastic soil stiffness at the base of an individual pile i in an n_p-pile group, f_g, can be calculated as:

$$f_g = \frac{1}{k_{bi}} \tag{38}$$

The value of parameter, g_g, presented in the hyperbolic model of end resistance of an individual pile i in an n_p-pile group can be taken as identical to the value of b of a hyperbolic model of end resistance of a single pile obtained from equation (18).

Based on the above suggested determinations of the parameters presented in the hyperbolic model of an individual pile in a pile group and the previously proposed iterative computer program developed for the analysis of

the response of a single pile, the conventional load-transfer approach can be extended to the analysis of the load-settlement response of an arbitrary pile in a pile group.

5. Case Studies on Pile Group Response

To check the reliability of the proposed method for the analysis of the load-settlement response of a pile group, the approach described in this paper is applied to analyze two field loading tests on pile groups previously reported by O'Neill et al. [34] and Briaud et al. [35] in case one and case two, respectively.

5.1. Case one

The first case history was reported by O'Neill et al. [34] on closed-ended steel pipe piles driven in stiff overconsolidated clays as previously descried. In the analysis of the response of a pile group, the Poisson's ratio of the soil is adopted as 0.5. The values of R_{sf} and R_{bf} are adopted as 0.90 for the whole deposit around pile shaft and the soil below the pile toe, respectively. The values of a_g and b_g are calculated using equations (33) and (14), respectively, while the values of f_g and g_g can be computed by equations (37) and (18), respectively. The load-settlement responses of the four-pile group and the nine-pile group can be calculated using the parameters a_g, b_g, f_g and g_g of the hyperbolic model of an individual pile in a pile group and the previously proposed iterative computer program developed for the analysis of a single pile response.

Fig.9 compares the measured load-average settlement behavior of the nine-pile group and four-pile subgroup with the computed values. At low loading level, very good agreement between the measured values given by O'Neill et al. [34], the computed results suggested by Castelli and Maugeri [36], and the calculated results estimated from the present approach is generally observed. At about one-half of the ultimate load, the results predicted by the proposed method are slightly larger than the observed behavior and the computed values given by Castelli and Maugeri.
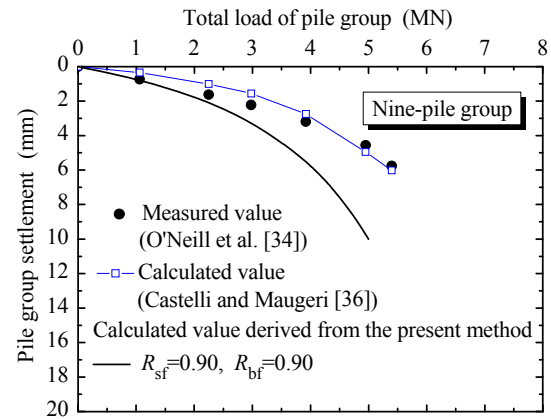
Fig. 9 Measured and calculated load-settlement curves at the pile head of the four-pile subgroup and the nine-pile group connected to a rigid reinforced concrete block

Comparing field test results in terms of pile head settlements, it is observed a general increasing of pile group settlements with respect to the case of single pile. The ratio between measured single pile and pile group settlement generally ranges around the average value of 0.80 for the case of four-pile subgroup and 0.62 for the case of nine-pile group (O'Neill et al. [34]). However, the ratio of calculated single pile to pile group settlement derived from the present method (R_{sf}=0.90 and R_{bf}=0.90) generally ranges around the average value of 0.55 and 0.45 for the case of four-pile subgroup and the case of nine-pile group, respectively (see Figs.5 and 9).

Table 4 shows the distribution of pile loads, predicted by the present method (R_{sf}=0.90, and R_{bf}=0.90), at the centre, edge, and corner piles at different loading levels in the nine-pile group connected to a rigid reinforced concrete block. For a pile group connected to a rigid reinforced concrete block, the largest, the second largest and the smallest pile loads are observed in the corner, edge, and centre piles, respectively. This is consistent with the field measured results and model test results (Cooke et al. [37]; Lee and Chung [38]).
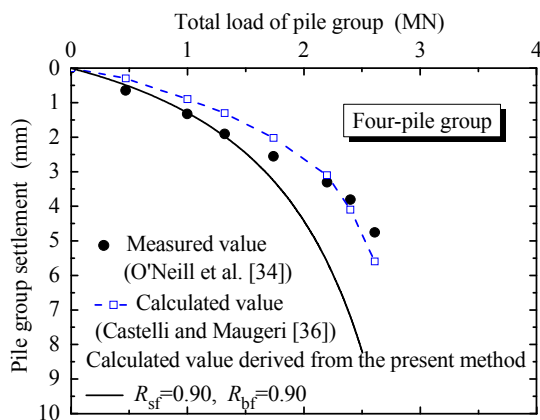
Table 4 Predicted pile head load at different locations in the nine-pile group connected to a rigid reinforced concrete block

Total applied load (kN)	Centre load (kN)	Edge load (kN)	Corner load (kN)	Settlement of nine-pile group (mm)
851.87	88.12	93.37	97.57	0.6
1327.59	138.21	145.73	151.61	1.0
2231.64	235.74	245.13	253.84	2.0
2865.43	305.56	314.37	325.59	3.0
3366.64	359.21	370.45	381.40	4.0
3783.04	404.79	416.46	428.10	5.0
4117.53	441.80	453.52	465.41	6.0
4397.42	472.53	484.13	497.09	7.0
4634.24	499.29	510.13	523.61	8.0
4847.65	523.10	534.01	547.13	9.0
5035.99	542.75	553.97	569.34	10.0
5192.12	561.15	571.02	586.72	11.0
5343.23	577.31	588.04	603.44	12.0

Fig. 10 shows the ratio of pile loads at the corner and edge piles to the centre pile head load at different levels of applied loads. The computed results indicates that the ratio of pile loads at the corner and edge piles to the centre pile head load decreases with increasing pile-group settlement (pile-group load) and tends to steady state.
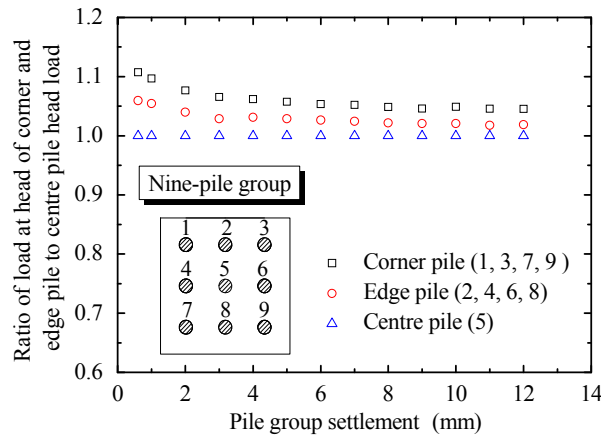
Fig. 10 Ratio of pile loads at the corner and edge piles to the centre pile head load at different levels of applied loads for the nine-pile group connected to a rigid reinforced concrete block

For a pile group connected to a flexible concrete block, the pile head loads can be assumed to be the same for all piles in the group. The load-settlement responses of the piles at different locations of the nine-pile group connected to a flexible concrete block can be predicted using the previously approach (R_{sf}=0.90, and R_{bf}=0.90), as shown in Fig. 11.

At the same loading level, the largest, the second largest and the smallest pile head settlements are observed at the centre, edge, and corner piles in the nine-pile group connected to a flexible concrete block, respectively. This discrepancy is probably caused by the development degree of the interactive effects for the individual piles at different pile locations. The interactive effect between individual piles developed at the centre pile is larger than the edge and corner piles.
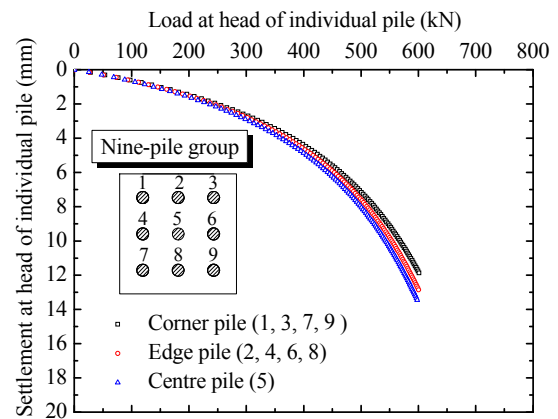
Fig. 11 Load-settlement responses of the piles at different locations of the nine-pile group connected to a flexible concrete block

5.2. Case two

The second case history reported by Briaud et al. [35] was performed on a five-pile group loaded to failure in a medium dense as descried earlier. In the analysis of the response of the five-pile group, the Poisson's ratio of the soil is adopted as 0.5. The values of R_{sf} and R_{bf} are adopted as 0.90 for the whole deposit around pile shaft and the soil below the pile toe, respectively. The values of a_g and b_g are calculated using equations (33) and (14), respectively, while the values of f_g and g_g can be computed by equations (37) and (18), respectively.

Fig.12 compares the measured load-average settlement response of the five-pile group with the computed values. The load-displacement curve at the pile head plotted from the present approach is generally consistent with the measured values given by Briaud et al. [35] and the computed results suggested by Castelli and Maugeri [36]. However, the discrepancies between the predicted and observed behavior generally becomes slightly larger when the piles approach their ultimate loads.

As above discussed, also in this case, it is observed a general increasing of pile group settlements with respect to the case of single pile. The ratio between measured single

Qian-qing Zhang, Shu-cai Li, Fa-yun Liang, Min Yang, Qian Zhang

pile and five-pile group settlement generally ranges around the average value of 0.70 (Briaud et al. [35]), while the ratio of calculated single pile to five-pile group settlement derived from the present method (R_{sf}=0.90 and R_{bf}=0.90) generally ranges around the average value of 0.80 (see Figs. 7 and 12).

Table 5 shows the distribution of pile loads, predicted by the present method (R_{sf}=0.90, and R_{bf}=0.90), at the centre and corner piles at different loading levels in the five-pile group connected to a rigid reinforced concrete block. It can be concluded that for a pile group connected to a rigid reinforced concrete block, the corner pile load is larger than the load applied at the centre pile.
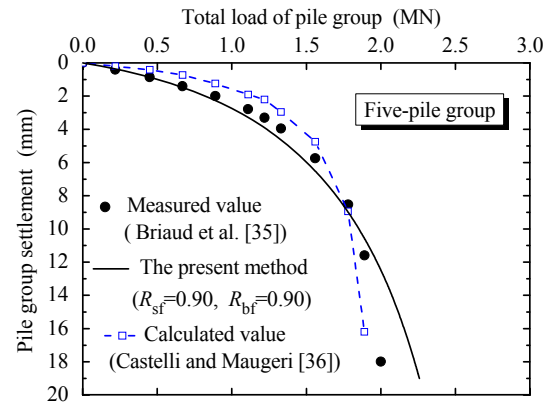
Fig. 12 Measured and calculated load-settlement responses of the five-pile group connected to a rigid reinforced concrete block

Table 5 Predicted pile head load at different locations in the five-pile group connected to a rigid reinforced concrete block

Total applied load (kN)	Centre load (kN)	Corner load (kN)	Settlement of five-pile group (mm)
550.44	101.86	112.17	1.0
876.30	162.47	178.46	2.0
1102.86	204.81	224.51	3.0
1279.61	237.65	260.49	4.0
1423.80	264.50	289.82	5.0
1557.22	289.48	316.94	6.0
1657.28	308.73	337.14	7.0
1747.27	325.60	355.42	8.0
1830.14	342.13	372.00	9.0
1902.15	356.76	386.35	10.0
1964.65	368.57	399.02	11.0
2022.89	380.43	410.61	12.0
2079.49	391.17	422.08	13.0
2118.82	399.99	429.71	14.0
2162.31	408.99	438.33	15.0
2201.95	417.26	446.17	16.0
2238.23	424.87	453.34	17.0
2271.58	431.90	459.92	18.0
2299.37	437.79	465.39	19.0
2328.06	443.91	471.04	20.0

Fig.13 shows the ratio of pile loads at the corner pile to the centre pile head load at different loading levels. The computed ratio of the corner pile head load to the load applied at the centre pile decreases with increasing pile-group settlement (pile-group load).

As previously discussed, the pile head loads can be assumed to be the same for all piles in the group connected to a flexible concrete block. The load-settlement responses of the corner and centre piles in the five-pile group connected to a flexible concrete block can be computed using the present method (R_{sf}=0.90, and R_{bf}=0.90), as shown in Fig.14.

Fig.14 shows that the pile head settlement of the centre pile is larger than that of the corner pile at the same loading level. The interactive effect between individual piles developed at the centre pile is larger than the corner piles. This will cause the discrepancy of the load-settlement response of the piles at different pile locations.
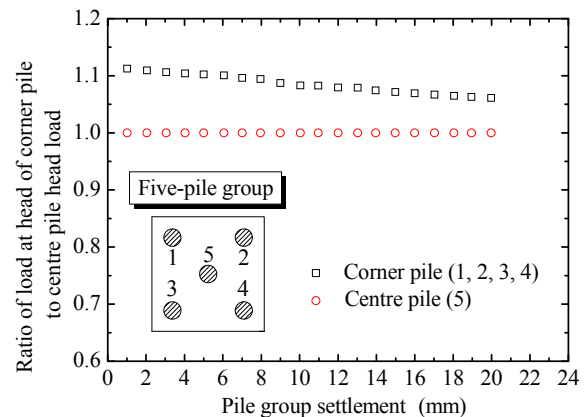
Fig. 13 Ratio of load at the head of corner pile to load at the top of centre pile for the five-pile group connected to a rigid reinforced concrete block
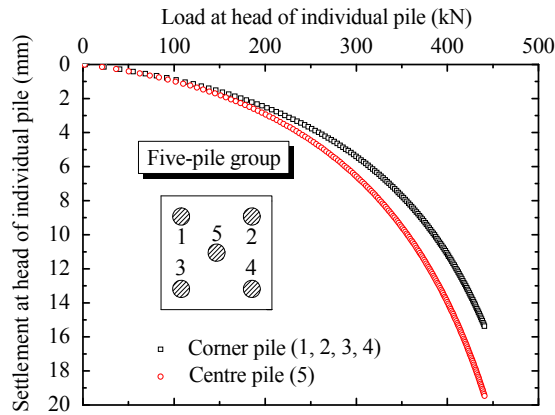
Fig. 14 Load-settlement response of corner and centre pile of the five-pile group connected to a flexible concrete block

6. Conclusions

In this work, a simplified approach for the nonlinear analysis of the load-displacement response of a single pile and a pile group is presented using the load-transfer approach. In the present method, a hyperbolic model is adopted to simulate the load-displacement response of both the pile base and the shaft. The reliability of the hyperbolic model of skin friction and end resistance is then demonstrated with the results of the load tests on instrumented piles. Based on the hyperbolic models, a highly effective iterative computer program is developed for the analysis of the response of a single pile. The calculated results indicate that the pile head displacement estimated from the present approach increases with increasing failure ratio of skin friction and end resistance at the same loading level.

Furthermore, determinations of the parameters presented in the hyperbolic model of skin friction and end resistance of an individual pile in a pile group are obtained considering interactions between piles. The conventional load-transfer approach can be extended to the analysis of the load-settlement response of an arbitrary pile in a pile group using the determinations of the parameters presented in the hyperbolic model of an individual pile and the proposed method developed for the analysis of a single pile response. Comparisons of the load-settlement response demonstrate that the proposed method is generally in good agreement with the well-documented field test results and the calculated results derived from other approaches. It can be concluded that at the same loading level, the largest, the second largest and the smallest pile head settlements are observed at the centre, edge, and corner piles in the nine-pile group connected to a flexible concrete block, respectively. This discrepancy is probably caused by the development degree of the interactive effects for the individual piles at different pile locations. The interactive effect between individual piles developed at the centre pile is larger than the edge and corner piles.

References

[1] Kraft L.M, Ray R.P, Kakaaki T. Theoretical t-z curves, Journal of the Geotechnical Engineering Division, 1981, Vol. 107, pp. 1543-1561.

[2] Zhang Q.Q, Zhang Z.M, He J.Y. A simplified approach for settlement analysis of single pile and pile groups considering interaction between identical piles in multilayered soils, Computers and Geotechnics, 2010, Vol. 37, pp. 969-976.

[3] Randolph M.F, Wroth C.P. An analysis of the vertical deformation of pile groups, Géotechnique, 1979, Vol. 29, pp. 423-439.

[4] Guo W.D, Randolph M.F. An efficient approach for settlement prediction of pile groups, Géotechnique, 1999, Vol. 49, pp. 161-179.

[5] Tosini L, Cividini A, Gioda G. A numerical interpretation of load tests on bored piles, Computers and Geotechnics, 2010, Vol. 37, pp. 425-430.

[6] Castelli F, Motta E. Settlement prevision of piles under vertical load, Proceedings of the ICE-Geotechnical Engineering, 1997, Vol. 156, pp. 183-191.

[7] Zhang Q.Q, Zhang Z.M. A simplified nonlinear approach for single pile settlement analysis, Canadian Geotechnical Journal, 2012, Vol. 49, pp. 1256-1266.

[8] Poulos H.G. Analysis of the settlement of pile groups, Géotechnique, 1968, Vol. 18, pp. 449-471.

[9] Lee C.Y. Settlement of pile group-practical approach, Journal of Geotechnical Engineering, 1993, Vol. 119, pp. 1449-1461.

[10] Comodromos E.M, Bareka S.V. Response evaluation of axially loaded fixed-head pile groups in clayey soils, International Journal for Numerical and Analytical Methods in Geomechanics, 1997, Vol. 33, pp. 839-1865.

[11] Mylonakis G, Gazetas G. Settlement and additional internal forces of grouped piles in layered soil, Géotechnique, 1998, Vol. 48, pp. 55-72.

[12] Chen S.L, Song C.Y, Chen L.Z. Two-pile interaction factor revisited, Canadian Geotechnical Journal, 2011, Vol. 48, pp. 754-766.

[13] Coyle H.M, Reese L.C. Load transfer for axially loaded piles in clay, Journal of the Soil Mechanics and Foundations Division, 1966, Vol. 92, pp. 1-26.

[14] Seed H.B, Reese L.C. The action of soft clay along friction piles, Transactions of the American Society of Civil Engineers, 1957, Vol. 122, pp. 731-754.

[15] Kezdi A. Pile foundations, In Foundation engineering handbook, Edited by H.F. Winterkorn, and H.Y. Fang, Van Nostrand Reinhold Company, Chapter 19, New York, 1975.

[16] Armaleh S, Desai C.S. Load deformation response of axially loaded piles, Journal of the Geotechnical Engineering Division, 1987, Vol. 113, pp. 1483-1499.

[17] Hirayama H. Load-settlement analysis for bored piles using hyperbolic transfer functions, Soils Found, 1990, Vol. 30, pp. 55-64.

[18] Lee K.M, Xiao Z.R. A simplified method for nonlinear analysis of single piles in multilayered soils, Canadian Geotechnical Journal, 2001, Vol. 38. pp. 1063-1080.

[19] Yang J, Tham L.G,. Lee P.K.K, Chan S.T, Yu F. Behavior of jacked and driven piles in sandy soil, Géotechnique, 2006, Vol. 56, pp. 245-259.

[20] Zhang Q.Q, Zhang Z.M, Yu F, Liu J.W. Field Performance of Long Bored Piles within Piled Rafts, Proceedings of the ICE - Geotechnical Engineering, 2010, Vol. 163, pp. 293-305.

[21] Zhang Z.M, Zhang Q.Q, Zhang G.X, Shi M.F. Large tonnage tests on super-long piles in soft soil area, Chinese Journal Of Geotechnical Engineering, 2011, Vol. 33, pp. 535-543. [in Chinese]

[22] Zhang Z.M, Zhang Q.Q, Yu F. A destructive field study on the behavior of piles under tension and compression, Journal of Zhejiang University SCIENCE A, 2011, Vol. 12, pp. 291-300.

[23] Clough G.W, Duncan J.M. Finite element analysis of retaining wall behavior, Journal of Geotechnical Engineering, 1971, Vol. 97, pp. 1657-1673.

[24] Kulhawy F.H. Limiting tip and side resistance: fact or fallacy, Analysis and design of pile foundations, Proceedings of a Symposium in conjunction with the ASCE National Convention, pp. 80-98, San Francisco, USA, 1984.

[25] Miller G.A, Lutenegger A.J. Influence of pile plugging on skin friction in overconsolidated clay, Journal of Geotechnical and Geoenvironmental Engineering, 1997, Vol. 123, pp. 525-533.

[26] O'Neill M.W, Raines R.D. Load transfer for pipe piles in highly pressured dense sand Journal of the Geotechnical Engineering Division, 1991, Vol. 117, pp. 1208-1226.

[27] Liu X.Z, Zhu H.H. Experiment on interaction between typical soils in Shanghai and concrete, Journal of Tongji University, 2004, Vol. 32, pp. 601-605. [in Chinese]

[28] Jardine R, Chow F, Overy R, Standing J. ICP design methods for driven piles in sands and clays, Thomas Telford, London, 2005.

[29] Ji L, Feng Z.X. Tests and analysis of piles socked in rock in Jiangyin Yangtze River highway bridge, In Pile Engineering Technology in High Rise Buildings, Edited by J.L. Liu, China Architecture & Building Press, pp. 416-420, Beijing, China, 1998. [in Chinese]

[30] Bi G.P, Su H.W, Gong W.M. Application of follow up grouting technology in slurry filling pile in Donghai Bridge engineering, In Pile Engineering Technology in High Rise Buildings, Edited by J.L. Liu, China Architecture & Building Press, pp. 575-581, Beijing, China, 2003. [in Chinese]

[31] Zhang Z.M, Xin G.F, Xia T.D. Test and research on unrock-socketed super-long pile in deep soft soil, China Civil Engineering Journal, 2004, Vol. 37, pp. 64-69. [in Chinese]

[32] Yao J.Y, Yu K, Ma Y.G. Self-balanced load test for carrying capacity of foundation piles of Songhua river bridge in Harbin, Bridge Constr, 2007, Vol. S1, pp. 135-137. [in Chinese]

[33] Cheng Y, Gong W.M, Zhang X.G, Dai G.L. Experimental research on post grouting under super-long and large-diameter bored pile tip, Chinese Journal of Rock Mechanics and Engineering, 2010, Vol. 29, pp. 3885-3892. [in Chinese]

[34] O'Neill M.W, Hawkins R.A, Mahar L.J. Load transfer mechanisms in piles and pile groups, Journal of the Geotechnical Engineering Division, 1982, Vol. 108, pp. 1605-1623.

[35] Briaud J. L, Tucker L. M, Ng E. Axially loaded 5 pile group and single pile in sand, Proceedings of the 12th International Conference on Soil Mechanics and Foundation Engineering, 1989, Vol. 2, pp. 1121-1124, Rio de Janeiro, Brazil.

[36] Castelli F, Maugeri M. Simplified nonlinear analysis for settlement prediction of pile groups, Journal of Geotechnical and Geoenvironmental Engineering, 2002, Vol. 128, pp. 76-84.

[37] Cooke R.W, Price G, Tarr K.W. Jacked piles in London clay: interaction and group behavior under working conditions, Géotechnique, 1980, Vol. 30, pp. 449-471.

[38] Lee S.H, Chung C.K. An experimental study of the interaction of vertically loaded pile groups in sand, Canadian Geotechnical Journal, 2005, Vol. 42, pp. 1485-1493.